Proceeding of the 2004 American Control Conference
Boston, Massachusetts June 30 - July 2, 2004

Nonlinear Sliding Mode Control and Feasible Workspace Analysis for a Cable Suspended Robot with Input Constraints and Disturbances

So-Ryeok Oh and Sunil Kumar Agrawal

***Abstract*— This paper deals with the characterization of the feasible workspace of set-point control for a cable suspended robot. The motivation behind this work is to find admissible set points for the system under disturbances as well as input constraints. The main ideas are: (i) designing a sliding mode controller as a stabilizing controller for the given uncertain system, (ii) finding the range of system states in terms of set points by analyzing the reaching condition and sliding mode, and (iii) substituting states in inequalities of the input with either their upper values or lower values so that constraints are satisfied. This method results in 6 inequalities in terms of set point which can be drawn graphically in the 3-dimensional space.**

I. INTRODUCTION

Cable driven robots are a class of robotic mechanisms which utilize multiple actuated cables to manipulate objects. Although there are many advantages to the use of cable robots, cables have a unique property - a cable can not provide compression force on an end-effector. This constraint leads to performance deterioration and even instability, if not properly accounted for in the design procedure.

The idea of redundancy has been used to satisfy the positive tension in the cables ([2],[3]). Based on the static modeling and geometry, approaches were suggested to determine the workspace ([1],[5],[6]).

In this paper, we propose a technique to estimate the admissible workspace of set-point control for a cable-suspended robot under disturbances. The computational procedure to obtain the admissible workspace consists of designing a stabilizing controller, calculating the range of system states in terms of set-points by solving the closed-loop system's dynamics, and replacing all the states in the constraints with their upper and lower values so that constraints are met. This procedure results in 6 inequlities for set-points, by which the feasible region can be sketched.

The remainder of this paper is organized as follows: Section II presents the kinematic and dynamic equations of the robot. The feedback controller based on Lyapunov method is outlined in Section III. In Section IV, we show how to characterize the feasible workspace of set-points in detail. The feasible workspace obtained by the proposed method is sketched in 3 dimensional space.

So-Ryeok Oh is a Graduate Student, Mechanical System Laboratory, Department of Mechanical Engineering, University of Delaware. oh@me.udel.edu

Sunil Kumar Agrawal is a Professor, Department of Mechanical Engineering, University of Delaware, Newark, DE 19716, USA. agrawal@me.udel.edu

II. SYSTEM DYNAMIC MODEL

A. End-effector Kinematics

Consider an inertial coordinate frame $\mathcal{F}_\mathcal{N}$ with origin O_N and basis vectors $\mathbf{n_1}, \mathbf{n_2}, \mathbf{n_3}$. The end-effector of the robot has a coordinate frame $\mathcal{F}_\mathcal{B}$ fixed to it with origin O and basis vectors $\mathbf{b_1}, \mathbf{b_2}, \mathbf{b_3}$. We choose the orientation of $\mathcal{F}_\mathcal{B}$ to be given by a space-three rotation sequence of ψ about $\mathbf{n_1}$, θ about $\mathbf{n_2}$, and ϕ about $\mathbf{n_3}$. A vector written in terms of coordinate frame $\mathcal{F}_\mathcal{B}$ can be written in terms of inertial frame using the rotation matrix, ${}^N R_B$ which is given as

$$ {}^N R_B = \begin{bmatrix} C\theta C\phi & S\psi S\theta C\phi - S\phi C\psi & C\psi S\theta C\phi + S\phi S\psi \\ C\theta S\phi & S\psi S\theta S\phi + C\phi C\psi & C\psi S\theta S\phi - C\phi S\psi \\ -S\theta & S\psi C\theta & C\psi C\theta \end{bmatrix}. \quad (1) $$

The position of O_B in $\mathcal{F}_\mathcal{N}$ is described by another three variables $(x_m, y_m, z_m)^T$ along three coordinate directions. These six variables are denoted by $\mathbf{x} = (x_m, y_m, z_m, \psi, \theta, \phi)^T$.

If the angular velocity of $\mathcal{F}_\mathcal{B}$ in $\mathcal{F}_\mathcal{N}$ is $\omega_1\mathbf{b_1}+\omega_2\mathbf{b_2}+\omega_3\mathbf{b_3}$, from rigid body kinematics,

$$ \begin{bmatrix} \omega_1 \\ \omega_2 \\ \omega_3 \end{bmatrix} = \begin{bmatrix} 1 & 0 & -S\theta \\ 0 & C\psi & S\psi C\theta \\ 0 & -S\psi & C\psi C\theta \end{bmatrix} \begin{bmatrix} \dot\psi \\ \dot\theta \\ \dot\phi \end{bmatrix} = P\dot{\mathcal{O}}, \quad (2) $$

where $\dot{\mathcal{O}} = (\dot\psi, \dot\theta, \dot\phi)^T$. If the angular acceleration of $\mathcal{F}_\mathcal{B}$ in $\mathcal{F}_\mathcal{N}$ is $\alpha_1\mathbf{b_1} + \alpha_2\mathbf{b_2} + \alpha_3\mathbf{b_3}$, then

$$ \begin{bmatrix} \alpha_1 \\ \alpha_2 \\ \alpha_3 \end{bmatrix} = \dot P\dot{\mathcal{O}} + P\ddot{\mathcal{O}}. \quad (3) $$

If we define the position of O_B in $\mathcal{F}_\mathcal{N}$ as $(x_m, y_m, z_m)^T$, the configuration of the end-effector plate is given by $\mathbf{x} \triangleq [x_m, y_m, z_m, \psi, \theta, \phi]^T$.

B. Kinematics and Statics

Fig. 1 shows the cable attachment points D, E, F on the end-effector and A, B, C in the inertial frame. The coordinates of cable attachment points D, E, F can be written in terms of $\mathbf{x}$ and geometric parameters of the end-effector. Similarly, the coordinates of attachment points A, B, C of the cables are also known in $\mathcal{F}_\mathcal{N}$. Using the coordinates of the two end-points of a cable, the length q_i of cable i is given by

$$ q_i = q_i(\mathbf{x}),\ i = 1, \cdots, 6. \quad (4) $$

0-7803-8335-4/04/$17.00 ©2004 AACC

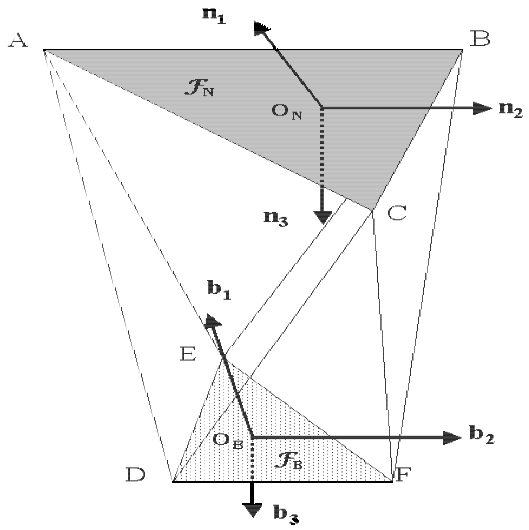

Fig. 1. A sketch of the cable system along with geometric parameters.

On defining $\mathbf{q} \triangleq [q_1, q_2, \cdots, q_6]^T$, the position kinematics of the robot is captured in the following nonlinear map

$$\mathbf{q} = \mathbf{q}(\mathbf{x}). \tag{5}$$

With the velocity of the reference point defined as $\dot{x}_m\mathbf{n_1} + \dot{y}_m\mathbf{n_2} + \dot{z}_m\mathbf{n_3}$ and angular velocity of $\mathcal{F}_\mathcal{B}$ as $\omega_1\mathbf{b_1} + \omega_2\mathbf{b_2} + \omega_3\mathbf{b_3}$, both with respect to the inertial reference frame,

$$\dot{\mathbf{q}} = \tilde{J}(\dot{x}_m, \dot{y}_m, \dot{z}_m, \omega_1, \omega_2, \omega_3)^T, \tag{6}$$

where $\tilde{J}$ is (6×6) matrix and is the *inverse Jacobian* map for the robot. It is also well known that there is a dual relation between externally applied wrench on the end-effector and the cable tensions required to keep the system in equilibrium, This relationship is

$$(F_x, F_y, F_z, M_1, M_2, M_3)^T = -\tilde{J}^T\mathbf{u}, \tag{7}$$

where the external force on the end-effector at the reference point is $F_x\mathbf{n_1} + F_y\mathbf{n_2} + F_z\mathbf{n_3}$ and the external moment on the end-effector plate is given by $M_1\mathbf{b_1} + M_2\mathbf{b_2} + M_3\mathbf{b_3}$. Here, $\mathbf{u}$ is the vector of cable tensions. A positive cable tension u_i is in opposite direction to the cable elongation q_i. Through simple substitution, it can be shown that the gradient of Eqn. (5) and $\tilde{J}$ are related in the following way:

$$J = [\,\tfrac{\partial \mathbf{q}}{\partial \mathbf{x}}\,] = \tilde{J}\begin{bmatrix} I_3 & 0 \\ 0 & P \end{bmatrix}, \tag{8}$$

where I_3 is a (3×3) identity matrix, and P is the 3×3 matrix defined in Eqn. (2).

C. Dynamic Equations of Motion

On using Newton-Euler's laws, the equations of motion can be written in the following form.

$$\begin{bmatrix} m\ddot{x}_m \\ m\ddot{y}_m \\ m(\ddot{z}_m - g) \\ I\begin{pmatrix}\alpha_1\\ \alpha_2\\ \alpha_3\end{pmatrix} + \begin{pmatrix}\omega_1\\ \omega_2\\ \omega_3\end{pmatrix} \times I\begin{pmatrix}\omega_1\\ \omega_2\\ \omega_3\end{pmatrix} \end{bmatrix} - \tilde{\mathbf{d}}(t) = -\tilde{J}^T(\mathbf{q})\mathbf{u}, \tag{9}$$

where m is the mass and I is the moment of inertia of the end-effector about its center of mass with respect to the basis vectors $\mathbf{b_1}, \mathbf{b_2}, \mathbf{b_3}$, and $\tilde{\mathbf{d}}(t)$ is a disturbance vector on the end-effector. Again, we write the equations of motion in terms of $\mathbf{x}$ coordinates with the following general form:

$$M(\mathbf{x})\ddot{\mathbf{x}} + C(\mathbf{x}, \dot{\mathbf{x}})\dot{\mathbf{x}} + \mathbf{g}(\mathbf{x}) = -J^T(\mathbf{q})\mathbf{u} + \mathbf{d}(t) \tag{10}$$

where,

$$\begin{aligned} M(\mathbf{x}) &= \begin{bmatrix} mI_3 & 0 \\ 0 & P^T I P \end{bmatrix}, \\ C(\mathbf{x}, \dot{\mathbf{x}})\dot{\mathbf{x}} &= \begin{bmatrix} 0 \\ P^T\left\{I\dot{P}\dot{\mathcal{O}} + (P\dot{\mathcal{O}}) \times I(P\dot{\mathcal{O}})\right\} \end{bmatrix}, \\ \mathbf{g}(\mathbf{x}) &= \begin{bmatrix} 0 \\ 0 \\ -mg \\ 0_3 \end{bmatrix}, \quad \mathbf{d}(t) = \begin{bmatrix} I_3 & 0 \\ 0 & P^T \end{bmatrix}\tilde{\mathbf{d}}(t) \end{aligned} \tag{11}$$

where 0_3 is a (3×1) zero vector.

III. Feedback Controller

A. Sliding Mode Controller

We implement the sliding mode controller for the set-point control of the end-effector and show how to obtain the admissible range of the set-points that ensures positive cable tension during motion. First of all, we define a sliding surface and a Lyapunov function in the following equations.

$$\mathbf{s}_{6\times 1} = \dot{\mathbf{x}} + \mathbf{\Lambda}(\mathbf{x} - \mathbf{x}_d)\ , \tag{12}$$

$$V = \frac{1}{2}\mathbf{s}^T\mathbf{s}\ , \tag{13}$$

and $\Lambda = \begin{bmatrix} \lambda_1 & & O \\ & \ddots & \\ O & & \lambda_6 \end{bmatrix}$.

Differentiating Eq. (13) w.r.t. time leads to

$$\begin{aligned} \dot{V} &= \mathbf{s}^T\dot{\mathbf{s}}\ , \\ &= \mathbf{s}^T[\ddot{\mathbf{x}} + \Lambda\dot{\mathbf{x}}]\ , \\ &= \mathbf{s}^T[M^{-1}(\mathbf{x})(-J^T(\mathbf{x})\mathbf{u} + \mathbf{d}(t) \\ &\qquad - C(\mathbf{x}, \dot{\mathbf{x}})\dot{\mathbf{x}} - \mathbf{g}(\mathbf{x})) + \Lambda\dot{\mathbf{x}}]. \end{aligned} \tag{14}$$

To make $\dot{V}$ negative, we select the control law as

$$\begin{aligned} \mathbf{u} = -(J^T)^{-1}[&C(\mathbf{x}, \dot{\mathbf{x}})\dot{\mathbf{x}} + \mathbf{g}(\mathbf{x}) \\ &+ M(\mathbf{x})(-\Lambda\dot{\mathbf{x}} - Ksgn(\mathbf{s})]\ , \end{aligned} \tag{15}$$

where $K = \begin{bmatrix} k_1 & & O \\ & \ddots & \\ O & & k_6 \end{bmatrix}$ is diagonal matrix and $sgn(\mathbf{s}) = \begin{bmatrix} sgn(s_1) \\ \vdots \\ sgn(s_6) \end{bmatrix}$. This leads to

$$\begin{aligned} \dot{V} &= \mathbf{s}^T[M(\mathbf{x})^{-1}(\mathbf{x})\mathbf{d}(t) - Ksgn(\mathbf{s})] \ , \\ &\leq \sum_{i=1}^{6} |s_i|(\sum_{j=1}^{6} |(M(\mathbf{x})^{-1})_{ij}|f_j - k_i) \ , \\ &= -\sum_{i=1}^{6} \eta_i |s_i| \ . \end{aligned} \tag{16}$$

where $k_i = \sum_{j=1}^{6} |(M(\mathbf{x})^{-1})_{ij}|f_j + \eta_i$, $\underline{\eta} = [\eta_1, \cdots, \eta_6]^T$, and $|d_i(t)| \leq f_i, \ i = 1, \cdots, 6$. The total energy decreases since $\dot{V} \leq 0$ and the invariant set that satisfies $\dot{V} = 0$ has only $s_i = 0 \ , \ i = 1, \cdots, 6$, as its canditates. Hence, there does not exist any other points where system will get stuck. Hence, the equilibrium at $\mathbf{x}_d$ is globally asymptotically stable as long as cables are in tension during motion.

B. Bounds on states

We calculate the bounds on states $\mathbf{x}$ and $\ddot{\mathbf{x}}$ in terms of set points $\mathbf{x}_d$ for the cable robot with the stabilizing controller. This will be used to check the admissibility of set-point for system constraints in the following section. Starting from an initial condition, the state trajectory reaches a slide surface ($\mathbf{s} = 0$) in a finite time, and then slides along the surface towards $\mathbf{x}_d$ exponentially, with a time-constant equal to $1/\lambda$.

Under the assumptions $\mathbf{x}(0) = \mathbf{x}_0, \ \dot{\mathbf{x}}(0) = 0$, and $\mathbf{x}_0 \leq \mathbf{x}_d$, $\mathbf{s}_0$ is placed in the region of $\mathbf{s} < 0$. We will show that the states of the system are governed by $\dot{\mathbf{s}} \geq \eta$ until they reach the sliding surface $\mathbf{s} = 0$. The calculation procedure to find the range of states then will depend on the cases: (i) reaching phase with $\dot{\mathbf{s}} \geq \eta$, (ii) and sliding phase $\mathbf{s} = 0$. In addition, we need to know the upper bound of $\dot{\mathbf{s}}$ to determine the interval of states precisely. From Eq. (16), we get the equation for $\dot{\mathbf{s}}$ as follows

$$\begin{aligned} \dot{\mathbf{s}} &= M^{-1}(\mathbf{x})\mathbf{d}(t) - Ksgn(\mathbf{s}) \ , \\ &= \begin{bmatrix} \sum_{j=1}^{6} (M^{-1}(\mathbf{x}))_{1j} d_j \\ \vdots \\ \sum_{j=1}^{6} (M^{-1}(\mathbf{x}))_{6j} d_j \end{bmatrix} + \begin{bmatrix} \sum_{j=1}^{6} |(M^{-1}(\mathbf{x}))_{1j}|f_j \\ \vdots \\ \sum_{j=1}^{6} |(M^{-1}(\mathbf{x}))_{6j}|f_j \end{bmatrix} + \underline{\eta}. \end{aligned} \tag{17}$$

Since $|d_i| \leq f_i \ , i = 1, \cdots, 6$, we can find the bounds of $\dot{\mathbf{s}}$ as

$$\eta \leq \dot{\mathbf{s}} \leq \underbrace{2 \begin{bmatrix} \sum_{j=1}^{6} |(M^{-1}(\mathbf{x}))_{1j}|f_j \\ \vdots \\ \sum_{j=1}^{6} |(M^{-1}(\mathbf{x}))_{6j}|f_j \end{bmatrix}}_{\Delta\underline{\eta}} + \underline{\eta}, \tag{18}$$

Similarily, in case of $\mathbf{s}_0 > 0$, we can derive the limitation of $\dot{\mathbf{s}}$ as

$$-\Delta\underline{\eta} - \underline{\eta} \leq \dot{\mathbf{s}} \leq -\underline{\eta} \tag{19}$$

In order to make $M(\mathbf{x})$ a constant matrix, we focus on the case when $[\psi, \theta] = [0, 0]$. For such a case, $M(\mathbf{x})$ becomes a diagonal matrix $M = diag(m, m, m, I_1, I_2, I_3)$. $[\psi, \theta]$ remain at zero during the motion by setting $[\psi_d, \theta_d] = [0, 0]$ and $[\psi_0, \theta_0] = [0, 0]$ due to the nature of the stabilizing controller. In this case, $\Delta\underline{\eta}$ and $\mathbf{k}$ become

$$\Delta\underline{\eta} = 2 \ [\ \frac{f_1}{m} \ , \ \frac{f_2}{m} \ , \ \frac{f_3}{m} \ , \ \frac{f_4}{I_1} \ , \ \frac{f_5}{I_2} \ , \ \frac{f_6}{I_3} \ ]^T \tag{20}$$

and $\mathbf{k} = \frac{1}{2}\Delta\underline{\eta} + \underline{\eta}$, where $\mathbf{k} = [k_1, \cdots, k_6]^T$.

In summary, $\dot{\mathbf{s}}$ has an upper bound as well as a lower bound

$$\underline{\eta}_m \leq \dot{\mathbf{s}} \leq \underline{\eta}_M \ , \tag{21}$$

where $\underline{\eta}_m = \underline{\eta}, \ \underline{\eta}_M = \Delta\underline{\eta} + \underline{\eta}$. Note that they are state independent, or constant vectors. Using Eq. (12), we can express Eq. (21) in terms of derivatives of $\mathbf{x}$ as

$$\underline{\eta}_m \leq \ddot{\mathbf{x}} + \Lambda\dot{\mathbf{x}} \leq \underline{\eta}_M \ . \tag{22}$$

Without using index, we define i^{th} inequality in Eq. (22) as

$$\eta_m \leq \ddot{x} + \lambda\dot{x} \leq \eta_M \ . \tag{23}$$

Given initial conditions ($x_0, \dot{x}_0 = 0$), we can solve the equation $\ddot{x} + \lambda\dot{x} = \eta$, such that $\eta_m \leq \eta \leq \eta_M$, to result in

$$\begin{bmatrix} x \\ \dot{x} \\ \ddot{x} \end{bmatrix} = \begin{bmatrix} x_0 + \frac{\eta}{\lambda}t + \frac{\eta}{\lambda^2}(1 - e^{-\lambda t}) \\ \frac{\eta}{\lambda}(1 - e^{-\lambda t}) \\ \eta e^{-\lambda t} \end{bmatrix}. \tag{24}$$

Let's define x_s and t_s as the value of x and the corresponding time on arrival at the sliding surface. Hence, x_s should satisfy $s = 0$, or $\dot{x}_s + \lambda(x_s - x_d) = 0$, which gives $x_s < x_d$ since $\dot{x}_s > 0$ from Eq. (24). Also, as well known [7], $t_s = -\frac{s_0}{\eta}$. From Eq. (24), we observe that x keeps increasing towards x_s because of $\dot{x} > 0$ and $\ddot{x}$ varies over $[\eta e^{-\lambda t_s} \ , \eta]$. Referring to $\eta_m \leq \eta \leq \eta_M$, we can know that

$$\begin{aligned} x &\in \ [\ x_0 \ , \ max(x_s^m, x_s^M \ ) \ ] \\ \ddot{x} &\in \ [\ \eta_m e^{-\lambda t_s^m} \ , \ \eta_M \ ], \end{aligned} \tag{25}$$

where x_s^i, t_s^i is the reaching state and time governed by $\dot{s} = \eta_i \ , \ i = m, M$, respectively.

Next, we look into the behavior on the sliding surface $s = 0$. With an initial value x_s(*reaching state*), we can solve for $s = 0$, or $\dot{x} + \lambda(x - x_d) = 0$. This gives us simple solutions as

$$\begin{bmatrix} x \\ \dot{x} \\ \ddot{x} \end{bmatrix} = \begin{bmatrix} x_d + (x_s - x_d)e^{-\lambda(t - t_s)} \\ -\lambda_(x_s - x_d)e^{-\lambda(t - t_s)} \\ \lambda^2(x_s - x_d)e^{-\lambda(t - t_s)} \end{bmatrix} \tag{26}$$

$\ddot{x}$ varies over $[\lambda^2(x_s - x_d), \ 0]$. x_s continues to increase towards x_d along the sliding surface without overshoot,

which means that x keeps on increasing from x_0 to x_d during the motion. Combining solutions from the reaching phase and the sliding phase leads us to find the overall range of $x,\ \ddot{x}$ as follows :

$$\begin{aligned} x &\in \overbrace{[x_0,\ \ max(x_s^m, x_s^M\ )]}^{\dot{s}=\eta} \ \cup\ \overbrace{[\ x_s\ ,\ \ x_d]}^{s=0}\ , \\ \ddot{x} &\in \overbrace{[\eta_m e^{-\lambda t_s^m},\ \ \eta_M]}^{\dot{s}=\eta} \ \cup\ \overbrace{[\lambda^2(x_s - x_d),\ \ 0]}^{s=0}, \end{aligned} \tag{27}$$

which gives

$$\begin{aligned} x &\in [\ x_0 \quad x_d]\ , \\ \ddot{x} &\in [\lambda^2(x_s - x_d),\ \ \eta_M]\ . \end{aligned} \tag{28}$$

In addition, $\ddot{x} \in [\lambda^2(x_0 - x_d),\ \eta_M]$ since $x_0 < x_s$. Hence, we successfully obtained the range of the control state in terms of $x_0,\ x_d,\ \eta$, which will be used to do an analysis on the admissible region of set points in the following section.

IV. Feasible Workspace

Based on a quantitative analysis, we estimate the feasible workspace in the first octant ($\mathbf{x} > 0, \mathbf{y} > 0, \mathbf{z} > 0$) for a set-point control. In this paper, we deal with only two translational motions (z and $x-y$ motion) for want of space. This method can be used for determination on the feasible workspace in other octants.

A. Motion in z Direction

We search for the admissible region of set-points when the end-effector's initial and final configurations are set to $\mathbf{x}_0 = [0\ 0\ z_0\ 0\ 0\ 0]$ and $\mathbf{x}_d = [0\ 0\ z_d\ 0\ 0\ 0]$, where $z_0,\ z_d \geq 0$. Due to the fact that the states of the closed loop system converges to $\mathbf{x}_d$ exponentially, we can assure that during the motion the variables $x,\ y,\ \psi,\ \theta,\ \phi$ remain at zero. In other words, only z is in a motion without overshoot, ranging over $[z_0\ \ z_d]$. In this case, system matrices can be simplified as $M = diag(m,\ m,\ m,\ I_1,\ I_2,\ I_3)$, $C(\mathbf{x}, \dot{\mathbf{x}})\dot{\mathbf{x}} + \mathbf{g}(\mathbf{x}) = [0,\ 0,\ mg,\ 0,\ 0,\ 0]^T$, and

$$J(\mathbf{x}) = \begin{bmatrix} \frac{a+b}{\sqrt{3}c_{J1}} & \frac{a-2b}{\sqrt{3}c_{J2}} & \frac{a-2b}{\sqrt{3}c_{J2}} & \frac{a+b}{\sqrt{3}c_{J1}} & \frac{-2a+b}{\sqrt{3}c_{J3}} & \frac{-2a+b}{\sqrt{3}c_{J3}} \\ \frac{-a+b}{c_{J1}} & \frac{-a}{c_{J2}} & \frac{a}{c_{J2}} & \frac{a-b}{c_{J1}} & \frac{-b}{c_{J3}} & \frac{b}{c_{J3}} \\ \frac{-z}{c_{J1}} & \frac{-z}{c_{J2}} & \frac{-z}{c_{J2}} & \frac{-z}{c_{J1}} & \frac{-z}{c_{J3}} & \frac{-z}{c_{J3}} \\ \frac{bz}{c_{J1}} & 0 & 0 & \frac{-bz}{c_{J1}} & \frac{-bz}{c_{J3}} & \frac{bz}{c_{J3}} \\ \frac{-bz}{\sqrt{3}c_{J1}} & \frac{2bz}{\sqrt{3}c_{J2}} & \frac{2bz}{\sqrt{3}c_{J2}} & \frac{-bz}{\sqrt{3}c_{J1}} & \frac{-bz}{\sqrt{3}c_{J3}} & \frac{-bz}{\sqrt{3}c_{J3}} \\ \frac{2ab}{\sqrt{3}c_{J1}} & \frac{-2ab}{\sqrt{3}c_{J2}} & \frac{2ab}{\sqrt{3}c_{J2}} & \frac{-2ab}{\sqrt{3}c_{J1}} & \frac{2ab}{\sqrt{3}c_{J3}} & \frac{-2ab}{\sqrt{3}c_{J3}} \end{bmatrix}, \tag{29}$$

where $2a,\ 2b$ are respectively the dimension of triangular edges of the upper platform and end-effector. The expression for $c_{J1},\ c_{J2},\ c_{J3}$ are

$$\begin{aligned} c_{J1} &= \sqrt{\tfrac{(a+b)^2}{3} + (a-b)^2 + z^2}\ , \\ c_{J2} &= \sqrt{\tfrac{(a-2b)^2}{3} + a^2 + z^2}\ , \\ c_{J3} &= \sqrt{\tfrac{(2a-b)^2}{3} + b^2 + z^2}\ . \end{aligned} \tag{30}$$

Plugging system matrices shown above into Eqn. (10), we can solve Eqn. (10) w.r.t $\mathbf{u}$,

$$\mathbf{u} = -c_z(\ddot{z}(t) - g - \frac{d_z(t)}{m}) \begin{bmatrix} 1 \\ 1 \\ 1 \\ 1 \\ 1 \\ 1 \end{bmatrix}\ , \tag{31}$$

where the disturbance vector is given by $\mathbf{d}(t) = \tilde{\mathbf{d}}(t) = [0, 0, d_z(t), 0, 0, 0]^T$, $|d_z(t)| \leq f_z$ and $c_z = \frac{\sqrt{4b^2 - 4ba + 4a^2 + 3z(t)^2}}{6\sqrt{3}z(t)} > 0$, since $z(t) > 0$ during the motion. Therefore, the sign of $\mathbf{u}$ in Eqn. (31) is determined only by the terms in the parenthesis. Hence, the condition to make all the cable tensions positive is given as

$$-(\ddot{z} - g - \frac{\mathbf{d}_z(t)}{m}) \geq 0\ . \tag{32}$$

In the case of the downward motion ($z_0 < z_d$) of the end-effector, we know that $\ddot{z}$ is varying over $[\lambda_o^2(z_0 - z_d),\ \eta_{max,z}]$ from the result of the previous section. The determination of $\ddot{z}$ in Eqn. (32) should be made in such a way that LHS of the eqn. (32) is minimized. Using $max(\ddot{z}) = \eta_{max,z}$ and $min(\mathbf{d}_z(t)) = -f_z$ leads to

$$\begin{aligned} & -\eta_{max,z} + g + (-\tfrac{F_z}{m}) \ \geq 0\ , \\ \Rightarrow\ & -(2\tfrac{F_z}{m} + \eta_o) + g - \tfrac{F_z}{m} \ \geq 0\ , \\ \Rightarrow\ & \eta_o \leq g - \tfrac{3F_z}{m}\ , \end{aligned} \tag{33}$$

where $\eta = \eta_o\ [1, 1, 1, 1, 1, 1]^T$ and $\eta_{max,z} = 2\frac{F_z}{m} + \eta_o$. η_o that satisfies the condition in the eqn. (33) guarantees that the system is feasible for any set point z_d.

B. Motion in x-y Plane

In this section, we look into the feasible area of the set-points (x_d,y_d) on the x-y plane. The initial and final configuration is set to $\mathbf{z}_0 = [x_0,\ y_0,\ z_c,\ 0,\ 0,\ 0]$ and $\mathbf{z}_d = [x_d,\ y_d,\ z_c,\ 0,\ 0,\ 0]$. Here, $x_d > 0$, $y_d > 0$, $\mathbf{d}(t) = \tilde{\mathbf{d}}(t) = [D_x(t), D_y(t), 0, 0, 0, 0]^T$.

$$\mathbf{u} = \begin{bmatrix} c_{xy1}u_{xy1} \\ c_{xy2}u_{xy2} \\ c_{xy3}u_{xy3} \\ c_{xy4}u_{xy4} \\ c_{xy5}u_{xy5} \\ c_{xy6}u_{xy6} \end{bmatrix}\ , \tag{34}$$

where

$$\begin{aligned} u_{xy1} &= \sqrt{3}z_c\ddot{x} - z_c\ddot{y} + (\sqrt{3}x - y + a)g \\ &\quad -\sqrt{3}z_c\tfrac{d_x(t)}{m} + z_c\tfrac{d_y(t)}{m}\ , \\ u_{xy2} &= -2z_c\ddot{y} + (-2y + a)g + 2z_c\tfrac{d_y(t)}{m}\ , \\ u_{xy3} &= 2z_c\ddot{y} + (2y + a)g - 2z_c\tfrac{d_y(t)}{m}\ , \\ u_{xy4} &= \sqrt{3}z_c\ddot{x} + z_c\ddot{y} + (\sqrt{3}x + y + a)g \\ &\quad -\sqrt{3}z_c\tfrac{d_x(t)}{m} - z_c\tfrac{d_y(t)}{m}\ , \\ u_{xy5} &= -\sqrt{3}z_c\ddot{x} - z_c\ddot{y} + (-\sqrt{3}x - y + a)g \\ &\quad +\sqrt{3}z_c\tfrac{d_x(t)}{m} + z_c\tfrac{d_y(t)}{m}\ , \\ u_{xy6} &= -\sqrt{3}z_c\ddot{x} + z_c\ddot{y} + (-\sqrt{3}x + y + a)g \\ &\quad +\sqrt{3}z_c\tfrac{d_x(t)}{m} - z_c\tfrac{d_y(t)}{m}\ , \end{aligned} \tag{35}$$

and

$$
\begin{aligned}
c_{xy1} &= \frac{\sqrt{3}m}{18az_c}\sqrt{(\sqrt{3}x-a-b)^2+3(y+a-b)^2+3z_c^2},\\
c_{xy2} &= \frac{\sqrt{3}m}{18az_c}\sqrt{(\sqrt{3}x-a+2b)^2+3(y+a)^2+3z_c^2},\\
c_{xy3} &= \frac{\sqrt{3}m}{18az_c}\sqrt{(\sqrt{3}x-a+2b)^2+3(y-a)^2+3z_c^2},\\
c_{xy4} &= \frac{\sqrt{3}m}{18az_c}\sqrt{(\sqrt{3}x-a-b)^2+3(y+a+b)^2+3z_c^2},\\
c_{xy5} &= \frac{\sqrt{3}m}{18az_c}\sqrt{(\sqrt{3}x+2a-b)^2+3(y+b)^2+3z_c^2},\\
c_{xy6} &= \frac{\sqrt{3}m}{18az_c}\sqrt{(\sqrt{3}x+2a-b)^2+3(y-b)^2+3z_c^2}.
\end{aligned}
$$

Now, we can substitute $\ddot{x},\ \ddot{y},\ x$, and y in Eqn. (35) with either their minimum or maximum values in such a way that $u_{xyi},\ i=1,\cdots,6$ can be minimized as follows The procedure is

$$
\begin{aligned}
min(u_{xy1}) = \quad & \sqrt{3}z_c min(\ddot{x}) - z_c max(\ddot{y}) + (\sqrt{3}x_0 \\
& -y_d + a)g - \sqrt{3}z_c\tfrac{F_x}{m} + z_c\tfrac{(-F_y)}{m}\ .
\end{aligned}
$$

For $u_{xy1} \geq 0$, we get

$$
\begin{aligned}
& \sqrt{3}z_c[\lambda_o^2(x_0-x_d)] - z_c(2\tfrac{F_y}{m}+\eta_o) + \\
& (\sqrt{3}x_0 - y_d + a)g - \sqrt{3}z_c\tfrac{F_x}{m} - z_c\tfrac{F_y}{m} \geq 0\ , \\
& y_d \leq -\tfrac{\sqrt{3}z_c\lambda_o^2}{g}x_d + \tfrac{\sqrt{3}(z_c\lambda_o^2+g)}{g}x_0 \\
& -\tfrac{z_c\eta_o}{g} + a - \tfrac{z_c}{mg}(\sqrt{3}F_x + 3F_y)\ .
\end{aligned} \tag{36}
$$

$$
min(u_{xy2}) = \quad -2z_c max(\ddot{y}) - 2gy_d + ag + 2z_c\tfrac{(-F_y)}{m}\ .
$$

For $u_{xy2} \geq 0$, we get

$$
\begin{aligned}
& -2z_c(2\tfrac{F_y}{m}+\eta_o) - 2gy_d + ag - 2z_c\tfrac{F_y}{m} \geq 0\ , \\
& y_d \leq \tfrac{-3z_c}{mg}F_y - \tfrac{z_c\eta_o}{g} + \tfrac{a}{2}\ .
\end{aligned} \tag{37}
$$

$$
min(u_{xy3}) = \quad 2z_c min(\ddot{y}) + (2y_0 + a)g - 2z_c\tfrac{F_y}{m}\ .
$$

For $u_{xy3} \geq 0$, we get

$$
\begin{aligned}
& 2z_c[\lambda_o^2(y_0-y_d)] + (2y_0+a)g - 2z_c\tfrac{F_y}{m} \geq 0\ , \\
& y_d \leq \tfrac{z_c\lambda_o^2+g}{z_c\lambda_o^2}y_0 + \tfrac{ga}{2z_c\lambda_o^2} - \tfrac{F_y}{m\lambda_o^2}\ .
\end{aligned} \tag{38}
$$

$$
\begin{aligned}
min(u_{xy4}) = \quad & \sqrt{3}z_c min(\ddot{x}) + z_c min(\ddot{y}) + (y_0 + \sqrt{3}x_0 \\
& +a)g - \sqrt{3}z_c\tfrac{F_x}{m} - z_c\tfrac{F_y}{m}\ .
\end{aligned}
$$

For $u_{xy4} \geq 0$, we get

$$
\begin{aligned}
& \sqrt{3}z_c[\lambda_o^2(x_0-x_d)] + z_c[\lambda_o^2(y_0-y_d)] \\
& +(y_0 + \sqrt{3}x_0 + a)g - \sqrt{3}z_c\tfrac{F_x}{m} - z_c\tfrac{F_y}{m} \geq 0\ , \\
& y_d \leq -\sqrt{3}x_d + \tfrac{\sqrt{3}(z_c\lambda_o^2+g)}{z_c\lambda_o^2}x_0 + \tfrac{(z_c\lambda_o^2+g)}{z_c\lambda_o^2}y_0 \\
& +\tfrac{ag}{z_c\lambda_o^2} - \tfrac{(\sqrt{3}F_x+F_y)}{m\lambda_o^2}\ .
\end{aligned} \tag{39}
$$

$$
\begin{aligned}
min(u_{xy5}) = \quad & -\sqrt{3}z_c max(\ddot{x}) - z_c max(\ddot{y}) + (-\sqrt{3}x_d \\
& -y_d + a)g + \sqrt{3}z_c\tfrac{(-F_x)}{m} + z_c\tfrac{(-F_y)}{m}\ .
\end{aligned}
$$

For $u_{xy5} \geq 0$, we get

$$
\begin{aligned}
& -\sqrt{3}z_c(2\tfrac{F_x}{m}+\eta_o) - z_c(2\tfrac{F_x}{m}+\eta_o) \\
& +(-\sqrt{3}x_d - y_d + a)g - \sqrt{3}z_c\tfrac{F_x}{m} - z_c\tfrac{F_y}{m} \geq 0\ , \\
& y_d \leq -\sqrt{3}x_d - \tfrac{(\sqrt{3}+1)}{g}z_c\eta_o \\
& -\tfrac{3z_c}{mg}(\sqrt{3}F_x + F_y) + a\ .
\end{aligned} \tag{40}
$$

$$
\begin{aligned}
min(u_{xy6}) = \quad & -\sqrt{3}z_c max(\ddot{x}) + z_c min(\ddot{y}) + (-\sqrt{3}x_d \\
& +y_0 + a)g + \sqrt{3}z_c\tfrac{(-F_x)}{m} - z_c\tfrac{F_y}{m}\ .
\end{aligned}
$$

For $u_{xy6} \geq 0$, we get

$$
\begin{aligned}
& -\sqrt{3}z_c(2\tfrac{F_x}{m}+\eta_o) + z_c[\lambda_o^2(y_0-y_d)] \\
& +(-\sqrt{3}x_d + y_0 + a)g - \sqrt{3}z_c\tfrac{F_x}{m} - z_c\tfrac{F_y}{m} \geq 0\ , \\
=> \quad & y_d \leq -\tfrac{\sqrt{3}g}{z_c\lambda_o^2}x_d + \tfrac{z_c\lambda_o^2+g}{z_c\lambda_o^2}y_0 - \tfrac{\sqrt{3}\eta_o}{\lambda_o^2} \\
& -\tfrac{(3\sqrt{3}F_x+F_y)}{m\lambda_o^2} + \tfrac{ag}{z_c\lambda_o^2}\ .
\end{aligned} \tag{41}
$$

The feasible region can be sketched by the six linear inequalities given by Eqns. (36)-(41) for the first quadrant $(x>0, y>0)$.

V. Simulations

In this section, we sketch the feasible workspace obtained by the method described in the previous sections. The parameter values are listed in Table 1. In Table 1, $2a$ and

TABLE I

Simulation parameters

Parameter	Value	Parameter	Value
m	11.68	x_0	0
I_1	.58	y_0	0
I_2	.58	z_0	1
I_3	1.16	z_c	1
a	$47.28e^{-2}$	η_o	0.1
b	$14.85e^{-2}$	λ_o	0.1

$2b$ are the edge lengths of the upper platform and the end-effector respectively, I_i is the i^{th} diagonal entry of the end-effector's inertia matrix in the local frame.

A. Results

The feasible region was sketched using MAPLE **inequal** and **plot3d** function.

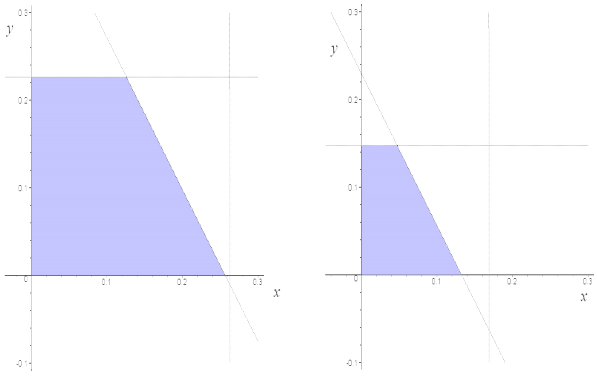

Fig. 2. Feasible workspaces of $x-y$ motion (LHS : $F_x = F_y = 0$, RHS: $F_x = F_y = 3[N]$)

1) The feasible regions obtained were different according to disturbaces on the end-effector. The disturbance reduced the feasible region of the set-points as depicted in Fig. 2-4.
2) In the case free of disturbances, the upper bound of the admissible region of y motion in Fig. 3 was similar to that of $x-y$ motion in Fig. 2 and the

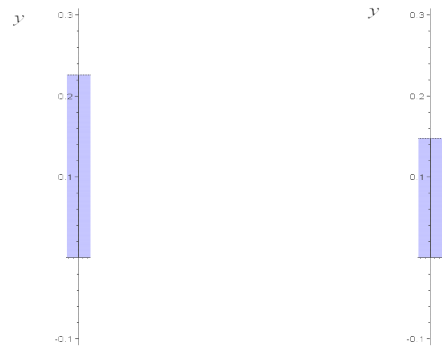

Fig. 3. Feasible workspaces of y motion (LHS : $F_y = 0$, RHS: $F_y = 3[N]$)

admissible maximum set-point of x motion in Fig. 4 was slightly less than that of $x-y$ motion in Fig. 2.

3) In Fig. 5, the feasible volume was bounded by two inequalities, u_{xyz3} and u_{xyz4}. In addition, the shape of a feasible area on the xy plane with $z = 1$ in Fig. 5 was similar to LHS plot of Fig. 2. In Fig. 5, the feasible area in xy plane decreased according to the increasing z.

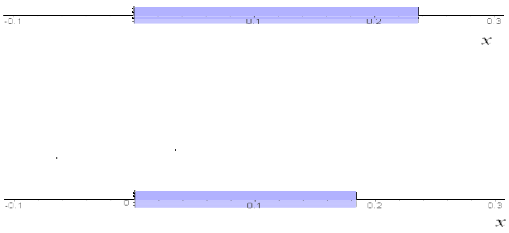

Fig. 4. Feasible workspaces of x motion (Upper : $F_x = 0$, Lower: $F_x = 3[N]$)

4) At $(x, y, z) = (0, 0, -)$ of Fig. 5, the value of z had a singularity. This fact comes from the results of Section 4.1: in z motion, the system is always safe for any selection of set-point z_d as long as the condition in the Section 4.1 is met. For the other octants($2^{nd} - 8^{th}$), we can apply the same method to determine the feasible workspace.

VI. Conclusion

This paper deals with the characterization of the feasible workspace for set point control of a cable-suspended robot under input constraints and disturbances. To do this, we implemented a sliding mode controller as a stabilizing controller for a given uncertain system and then we proposed a method to estimate the admissible workspace for

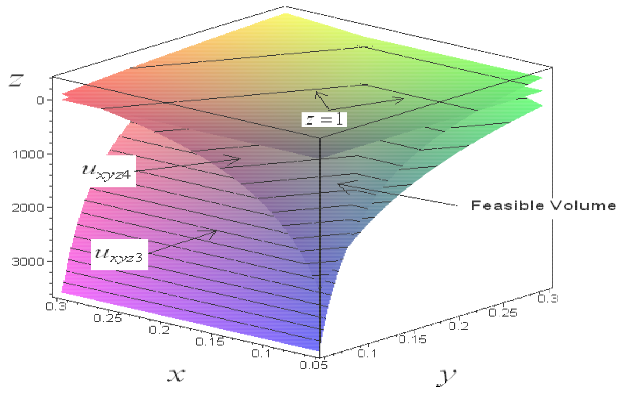

Fig. 5. Feasible workspaces of $x-y-z$ motion : $F_x = F_y = F_z = 0$

set-point control. The computational procedures to obtain the admissible workspace consist of calculating the range of system states during motion in terms of set-points by solving the reaching condition ($\dot{\mathbf{s}} > \eta$) and sliding mode ($\mathbf{s} = 0$) and replacing all the states in the control law with their upper and lower values in such a way that the positive input constraints are met. Inequalities obtained by the proposed method were sketched graphically to see the effect of the disturbances on the set-point's feasible region.

VII. Acknowledgments

The authors appreciate financial supports of NIST MEL Award No. 60NANB-2D0137, NSF Award No. IIS-0117733, PTI/NIST Award No. AGR20020506, and NIST Award No. SB 1341-03-W-0338.

References

[1] Robert, L., Williams II and Paolo Gallina, "Planar Cable-Direct-Driven Robots, Part I: Kinematics and Statics", *Proceedings of the 2001 ASME Design Technical Conferences 27TH Design Automation Conference*, DETC2001/DAC-21145, 2001.

[2] W. Shiang, D. Cannon, J. Gorman, "Dynamic Analysis of the Cable Array Robotic Crane", *Proceedings of the IEEE International Conference on Robotics and Automation*, Detroit, Michigan, 2495-2500, 1999.

[3] S. Oh, S. K. Agrawal, "Cable-Suspended Planar Parallel Robots with Redundant Cables: Controllers with Positive Cable Tensions", *Proceedings of the IEEE International Conference on Robotics and Automation*, Taipei, Taiwan, 3023-3028, 2003.

[4] Isidori, A. "Nonlinear Control Systems: an Introduction", *Berlin: Springer Verlag*, 1995.

[5] Y. Zheng, "Workspace Analysis of a Six DOF Wire-Driven Parallel Manipulator", *Proceedings of the WORKSHOP on Fundamental Issues and Future Research Derection for Parallel Mechanisms and Manipulators*, Quebec, Canada, 287-293, 2002.

[6] P. Lafourcade, M. Llibre, and C. Reboulet, "Design of a Parallel Wire-Driven Manipulator for Wind Tunnels", *Proceedings of the WORKSHOP on Fundamental Issues and Future Research Derection for Parallel Mechanisms and Manipulators*, Quebec, Canada, 187-293, 2002.

[7] Slotine, J.-J. E., and Weiping, L., "Applied Nonlinear Control", *Prentice Hall*, 1991.